



Fermi National Accelerator Laboratory

FERMILAB-Conf-89/168-T

August 9, 1989

The theory of heavy flavour production¹

R. K. Ellis

Fermi National Accelerator Laboratory

P. O. Box 500, Batavia, Illinois 60510

The theory of heavy quark production in hadronic reactions is reviewed. Rates for the production of charm, bottom and top quarks at energies of current interest are presented.



Operated by Universities Research Association Inc. under contract with the United States Department of Energy

¹Lectures given at the 17th SLAC Summer Institute, July 1989.

1. Lecture 1

1.1 The QCD parton model

The treatment of heavy quark production which I shall present relies on the QCD improved parton model. This model is generally applicable to high energy processes which involve a hard interaction. The parton model as originally envisaged by Feynman[1] provides a physical picture of a high energy scattering event in a frame in which the hadron is rapidly moving. In such a frame the hard interaction leading to the scattering event occurs on a time scale short compared to the scale which controls the evolution of the parton system. The characteristic evolution time for the parton system has been dilated by the Lorentz boost to the rapidly moving frame. During the hard interaction the partons can be treated as though they were effectively free. Only in such a frame does it make sense to talk about a number density of partons. The number of partons of type i with a momentum fraction between x and $x + dx$ is given by a distribution function $f_i(x)$.

Much of the structure of the parton model can be demonstrated to follow from the QCD Lagrangian, but with certain significant modifications. The QCD parton model has been introduced by Hinchliffe in his lectures[2]. I shall therefore only review the salient features of the model. The QCD parton model expresses the cross section σ for a hard scattering with characteristic momentum scale Q as follows,

$$\sigma(P_1, P_2) = \sum_{i,j} \int dx_1 dx_2 f_i(x_1, \mu) f_j(x_2, \mu) \hat{\sigma}_{ij}(\alpha_S(\mu), x_1 P_1, x_2 P_2) \quad (1.1)$$

This formula is illustrated in Fig. 1. The short distance cross section $\hat{\sigma}$ is evaluated at rescaled values of the incoming hadron momenta P_1 and P_2 . The sum on i and j runs over the light quarks and gluons. μ is an arbitrary scale which should be chosen to be of the order of the hard momentum scale Q . Note that the impulse approximation is used in Eq. 1.1. Interference terms which involve more than one active parton per hadron are not included. They require the transfer of the large momentum Q from one parton to another. Such interactions lead to terms which are suppressed by powers of the large scale Q and are not shown in Eq. 1.1.

The important features which distinguish QCD from the naive parton picture are as follows. The short distance cross section is now calculable as a systematic

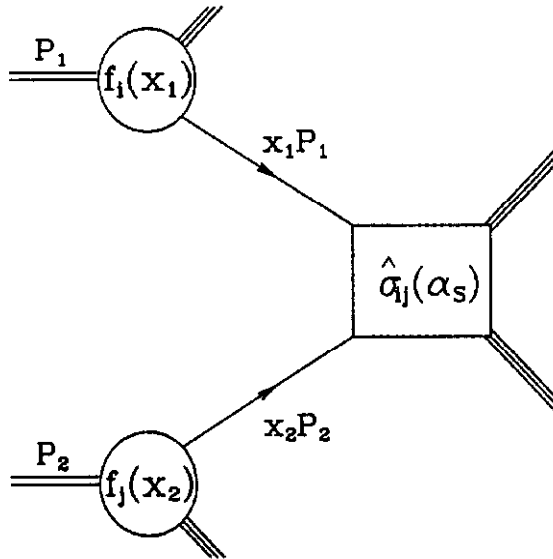


Figure 1: The parton model picture of a high energy scattering.

expansion in the strong coupling α_s because of the property of asymptotic freedom. The short distance cross section is defined to be the perturbatively evaluated parton cross section from which the mass singularities have been factorised. For details of this factorisation procedure I refer the reader to ref. [3]. The physical purpose of this procedure is to remove the long distance pieces (which are signalled by the presence of mass singularities) from the hard scattering cross section and place them in the parton distribution functions. The short distance cross section then contains only the physics of the hard scattering. In the Born approximation the short distance cross section is just the normal perturbatively calculated parton cross section, since no mass singularities occur in lowest order. The Born approximation is sufficient in many circumstances to extract the qualitative features of the physics predicted by the parton model. I shall therefore not explain the factorisation procedure in detail.

In QCD the parton distribution functions depend on scale μ in a calculable way as determined by the Altarelli-Parisi equation[4]. $f_i(x, \mu)$ is the number of partons in the infinite momentum frame carrying a fraction between x and $x + dx$ of the momentum of the incoming hadron and with a transverse size greater than $1/\mu$. The scale μ which occurs both in the running coupling and in the parton distributions and

should be chosen to be of the order of the hard interaction scale Q in order to avoid large logarithms in the perturbative expansion of the short distance cross section.

The doubly differential form of the parton model result will also be necessary for our purposes. Consider a hard scattering process in which two incoming hadrons of momenta P_1 and P_2 produce an observed final state with two partons of momenta p_3 and p_4 . The predicted invariant cross section is,

$$\frac{E_3 E_4 d\sigma}{d^3 p_3 d^3 p_4} = \sum_{i,j} \int dx_1 dx_2 f_i(x_1, \mu) f_j(x_2, \mu) \left[\frac{E_3 E_4 d\hat{\sigma}(\alpha_S(\mu), x_1 P_1, x_2 P_2)}{d^3 p_3 d^3 p_4} \right]. \quad (1.2)$$

I shall discuss the sensitivity of the physical predictions to the input parameters in detail in the second lecture. Suffice it to say at this point that the distributions of quarks and gluons in the proton are determined experimentally, mainly by the analysis of deeply inelastic lepton hadron scattering experiments. At present these experiments determine the form of the light quark distributions, and to a lesser extent the form of the gluon distribution function, in a range of $x \geq 10^{-2}$ and $\mu < 15$ GeV.

1.2 The theory of heavy quark production

The dominant parton reactions leading to the production of a sufficiently heavy quark Q of mass m are,

$$\begin{aligned} (a) \quad & q(p_1) + \bar{q}(p_2) \rightarrow Q(p_3) + \bar{Q}(p_4) \\ (b) \quad & g(p_1) + g(p_2) \rightarrow Q(p_3) + \bar{Q}(p_4), \end{aligned} \quad (1.3)$$

where the four momenta of the partons are given in brackets. The Feynman diagrams which contribute to the matrix elements squared in $O(g^4)$ are shown in Fig. 2. The justification of the use of perturbation theory in the calculation of heavy quark cross sections relies on the fact that all the propagators in Fig. 2 are off-shell by an amount at least m^2 . The invariant matrix elements squared [5,6] which result from the diagrams in Fig. 2 are given in Table 1. The matrix elements squared have been averaged (summed) over initial (final) colours and spins, (as indicated by $\overline{\sum}$). In order to express the matrix elements in a compact form, I have introduced the following notation for the ratios of scalar products,

$$\tau_1 = \frac{2p_1 \cdot p_3}{s}, \quad \tau_2 = \frac{2p_2 \cdot p_3}{s}, \quad \rho = \frac{4m^2}{s}, \quad s = (p_1 + p_2)^2 \quad (1.4)$$

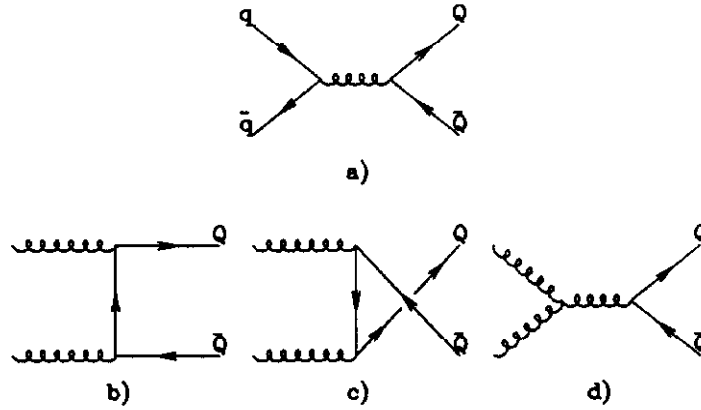


Figure 2: Lowest order Feynman diagrams for heavy quark production.

Process	$\sum M ^2$
$q \bar{q} \rightarrow Q \bar{Q}$	$\frac{V}{2N_c^2} \left(\tau_1^2 + \tau_2^2 + \frac{\rho}{2} \right)$
$g g \rightarrow Q \bar{Q}$	$\frac{1}{2VN_c} \left(\frac{V}{\tau_1\tau_2} - 2N_c^2 \right) \left(\tau_1^2 + \tau_2^2 + \rho - \frac{\rho^2}{4\tau_1\tau_2} \right)$

Table 1: Lowest order processes for heavy quark production. $\sum |M|^2$ is the invariant matrix element squared with a factor of g^4 removed. The colour and spin indices are averaged (summed) over initial (final) states.

The dependence on the $SU(N_c)$ colour group is shown explicitly, ($V = N_c^2 - 1$, $N_c = 3$) and m is the mass of the produced heavy quark Q .

In the Born approximation the short distance cross section is obtained from the invariant matrix element in the normal fashion[7].

$$d\hat{\sigma}_{ij} = \frac{1}{2s} \frac{d^3p_3}{(2\pi)^3 2E_3} \frac{d^3p_4}{(2\pi)^3 2E_4} (2\pi)^4 \delta^4(p_1 + p_2 - p_3 - p_4) g^4 \overline{\sum} |M_{ij}|^2 \quad (1.5)$$

The first factor is the flux factor for massless incoming particles. The other terms come from the phase space for two-to-two scattering.

I shall now illustrate why it is plausible that heavy quark production is described by perturbation theory[8]. Consider first the differential cross section. Let us denote the momenta of the incoming hadrons, which are directed along the z direction, by P_1 and P_2 and the square of the total centre of mass energy by S where $S = (P_1 + P_2)^2$. The short distance cross section in Eq. 1.2 is to be evaluated at rescaled values of the parton momenta $p_1 = x_1 P_1$, $p_2 = x_2 P_2$ and hence the square of the total parton centre of mass energy is $s = x_1 x_2 S$, if we ignore the masses of the incoming hadrons. The rapidity variable for the two final state partons is defined in terms of their energies and longitudinal momenta as,

$$y = \frac{1}{2} \ln \left[\frac{E + p_z}{E - p_z} \right]. \quad (1.6)$$

Using Eqs. 1.2 and 1.5 the result for the invariant cross section may be written as,

$$\frac{d\sigma}{dy_3 dy_4 d^2p_T} = \frac{\alpha_S^2(\mu)}{s^2} \sum_{ij} x_1 f_i(x_1, \mu) x_2 f_j(x_2, \mu) \overline{\sum} |M_{ij}|^2 \quad (1.7)$$

The energy momentum delta function in Eq. 1.5 fixes the values of x_1 and x_2 if we know the value of the p_T and rapidity of the outgoing heavy quarks. In the centre of mass system of the incoming hadrons we may write the components of the parton four momenta as $((E, p_x, p_y, p_z))$

$$\begin{aligned} p_1 &= \sqrt{S}/2(x_1, 0, 0, x_1) \\ p_2 &= \sqrt{S}/2(x_2, 0, 0, -x_2) \\ p_3 &= (m_T \cosh y_3, p_T, 0, m_T \sinh y_3) \\ p_4 &= (m_T \cosh y_4, -p_T, 0, m_T \sinh y_4) \end{aligned} \quad (1.8)$$

The transverse momentum in the final state has been arbitrarily routed along the x -direction. Applying energy and momentum conservation we obtain,

$$x_1 = \frac{m_T}{\sqrt{S}}(e^{y_3} + e^{y_4}), \quad x_2 = \frac{m_T}{\sqrt{S}}(e^{-y_3} + e^{-y_4}), \quad s = 2m_T^2(1 + \cosh \Delta y) \quad (1.9)$$

The transverse mass of the heavy quarks is denoted by $m_T = \sqrt{m^2 + p_T^2}$ and $\Delta y = y_3 - y_4$ is the rapidity difference between the two heavy quarks.

Using Eqs. 1.7 and 1.9, we may write the cross-section for the production of two massive quarks calculated in lowest order perturbation theory as,

$$\frac{d\sigma}{dy_3 dy_4 d^2 p_T} = \frac{\alpha_S^2(\mu)}{4m_T^4(1 + \cosh(\Delta y))^2} \sum_{ij} x_1 f_i(x_1, \mu) x_2 f_j(x_2, \mu) \overline{\sum} |M_{ij}|^2 \quad (1.10)$$

Expressed in terms of m, m_T and Δy the matrix elements for the two processes in Table 1 are,

$$\overline{\sum} |M_{q\bar{q}}|^2 = \frac{V}{2N_c^2} \left(\frac{1}{1 + \cosh(\Delta y)} \right) \left(\cosh(\Delta y) + \frac{m^2}{m_T^2} \right) \quad (1.11)$$

$$\overline{\sum} |M_{gg}|^2 = \frac{1}{VN_c} \left(\frac{V \cosh(\Delta y) - 1}{1 + \cosh(\Delta y)} \right) \left(\cosh(\Delta y) + 2\frac{m^2}{m_T^2} - 2\frac{m^4}{m_T^4} \right) \quad (1.12)$$

Note that, because of the specific form of the matrix elements squared, the cross section, Eq. 1.10, is strongly damped as the rapidity separation Δy between the two heavy quarks becomes large. It is therefore to be expected that the dominant contribution to the total cross section comes from the region $\Delta y \approx 1$.

I now consider the propagators in the diagrams shown in Fig. 2. In terms of the above variables they can be written as,

$$\begin{aligned} (p_1 + p_2)^2 &= 2p_1 \cdot p_2 = 2m_T^2(1 + \cosh \Delta y) \\ (p_1 - p_3)^2 - m^2 &= -2p_1 \cdot p_3 = -m_T^2(1 + e^{-\Delta y}) \\ (p_2 - p_3)^2 - m^2 &= -2p_2 \cdot p_3 = -m_T^2(1 + e^{\Delta y}) \end{aligned} \quad (1.13)$$

Note that the denominators are all off-shell by a quantity of least of order m^2 . It is this fact which distinguishes the production of a light quark from the production of a heavy quark. When a light quark is produced by these diagrams the lower cut-off on the virtuality of the propagators is provided by the light quark mass, which is less than the QCD scale Λ . Since propagators with small virtualities give the dominant

contribution, the production of a light quark will not be calculable in perturbative QCD. In the production of a heavy quark the lower cut-off is provided by the mass m . It is therefore plausible that heavy quark production is controlled by α_S evaluated at the heavy quark scale.

Note also that the contribution to the cross section from values of p_T which are much greater than the quark mass is also suppressed. The differential cross section falls like m_T^{-4} and as m_T increases the parton flux decreases because of the increase of x_1 and x_2 . Since all dependence on the transverse momentum appears in the transverse mass combination, the dominant contribution to the cross section comes from transverse momentum of the order of the mass of the heavy quark.

Thus for a sufficiently heavy quark we expect the methods of perturbation theory to be applicable. It is the mass of the heavy quark which provides the large scale in heavy quark production. The transverse momenta of the produced heavy quarks are of the order of the heavy quark mass and they are produced close in rapidity. The heavy quarks are produced predominantly centrally because of the rapidly falling parton fluxes. Final state interactions which transform the heavy quarks into the observed hadrons will not change the size of the cross section. A possible mechanism which might spoil this simple picture would be the interaction of the produced heavy quark with the debris of the incoming hadron. However these interactions with spectator partons are suppressed by powers of the heavy quark mass[9,10]. For a sufficiently heavy quark they can be ignored.

The theoretical arguments summarized above do not address the issue of whether the charmed quark is sufficiently heavy that the hadroproduction of charmed hadrons in all regions of phase space is well described by only processes (a) and (b) and their perturbative corrections.

Integrating Eq. 1.5 over all momenta we can obtain the total cross section for the production of a heavy quark. In general the total short distance cross section can be expressed as,

$$\hat{\sigma}_{ij}(s, m^2) = \frac{\alpha_S^2(\mu)}{m^2} \mathcal{F}_{ij}\left(\rho, \frac{\mu^2}{m^2}\right), \quad \alpha_S = \frac{g^2}{4\pi}. \quad (1.14)$$

Eq. 1.14 completely describes the short distance cross-section for the production of a heavy quark of mass m in terms of the functions \mathcal{F}_{ij} . The indices i and j specify the types of the annihilating partons. These short distance cross sections can be used

directly to predict the total heavy quark cross section using Eq. 1.1. The dimensionless functions \mathcal{F}_{ij} have a perturbative expansion in the coupling constant. The first two terms in this expansion can be expressed as follows,

$$\mathcal{F}_{ij}\left(\rho, \frac{\mu^2}{m^2}\right) = \mathcal{F}_{ij}^{(0)}(\rho) + 4\pi\alpha_S(\mu) \left[\mathcal{F}_{ij}^{(1)}(\rho) + \overline{\mathcal{F}}_{ij}^{(1)}(\rho) \ln\left(\frac{\mu^2}{m^2}\right) \right] + O(\alpha_S^2) \quad (1.15)$$

The energy dependence of the cross-section is given in terms of ρ and β ,

$$\rho = \frac{4m^2}{s}, \quad \beta = \sqrt{1 - \rho}. \quad (1.16)$$

The lowest order functions $\mathcal{F}_{ij}^{(0)}$ defined in Eq. 1.15 are obtained by integrating Eq. 1.5 using the results of Table 1. The results are,

$$\begin{aligned} \mathcal{F}_{q\bar{q}}^{(0)}(\rho) &= \frac{V\pi\beta\rho}{24N_c^2} \left[(2 + \rho) \right] \\ \mathcal{F}_{g\bar{g}}^{(0)}(\rho) &= \frac{\pi\beta\rho}{24VN_c} \left[3[\rho^2 + 2V(\rho + 1)]\mathcal{L}(\beta) + 2(V - 2)(1 + \rho) + \rho(6\rho - N_c^2) \right] \\ \mathcal{F}_{gq}^{(0)}(\rho) &= \mathcal{F}_{g\bar{q}}^{(0)}(\rho) = 0 \\ \mathcal{L}(\beta) &= \frac{1}{\beta} \ln\left(\frac{1 + \beta}{1 - \beta}\right) - 2 \end{aligned} \quad (1.17)$$

Note that the quark gluon process vanishes in lowest order, but is present in higher orders.

Using the results in Table 1 we can also calculate the average values of the transverse momentum squared. The $q\bar{q}$ contribution to the p_T^2 weighted cross section is,

$$\int dp_T^2 p_T^2 \frac{d\hat{\sigma}_{q\bar{q}}}{dp_T^2} = \frac{\alpha_S^2 \pi \beta^3 V}{60N_c^2} \left[3 + 2\rho \right] \quad (1.18)$$

and the gg contribution is

$$\begin{aligned} \int dp_T^2 p_T^2 \frac{d\hat{\sigma}_{gg}}{dp_T^2} &= \frac{\alpha_S^2 \pi \beta}{120VN_c} \left[2V \left[7\beta^2(2 + 3\rho) - 15\rho(1 + 2\rho)\mathcal{L}(\beta) \right] - 15\rho^3\mathcal{L}(\beta) \right. \\ &\quad \left. - 6(5\rho + 2)\beta^4 \right] \end{aligned} \quad (1.19)$$

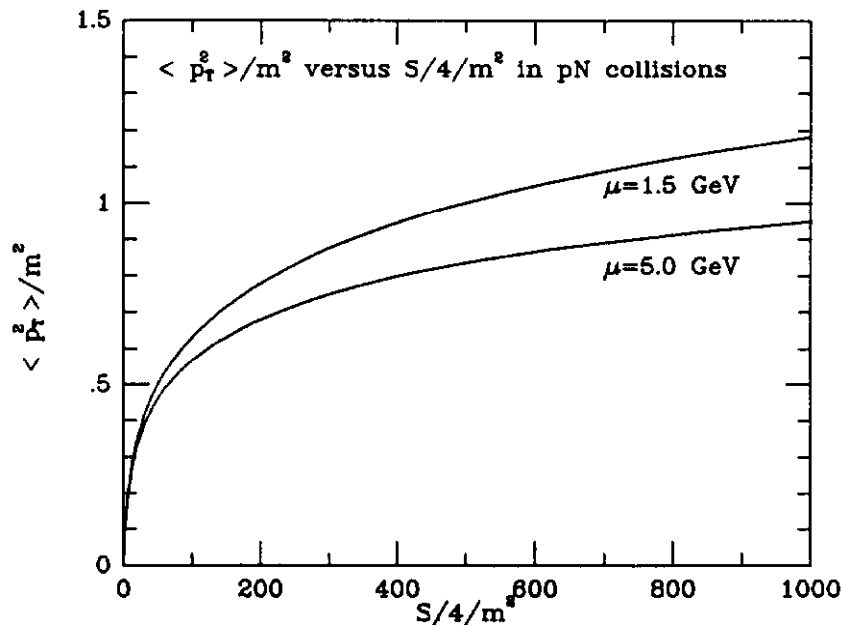


Figure 3: The average value of p_T^2 in heavy quark production.

with $\mathcal{L}(\beta)$ defined in Eq. 1.17. The results of Eqs. 1.14 and 1.17 allow us to calculate the average value of p_T^2 .

$$\langle p_T^2 \rangle = \frac{1}{\sigma} \int dp_T^2 p_T^2 \frac{d\sigma}{dp_T^2} \quad (1.20)$$

This leads to an average transverse momentum of order of the heavy quark mass. This is illustrated in Fig. 3 for the particular case of pN collisions. For all values of the beam energy which are sufficiently far above threshold to have a sizeable number of events, the average value of p_T^2 is of the order of m^2 . As shown in Fig. 3 p_T^2 continues to have a small dependence on μ , because of the μ dependence in the structure functions.

Far above threshold the average transverse momentum squared grows approximately linearly with \sqrt{S} .

$$\langle p_T^2 \rangle \approx m\sqrt{S} \quad (1.21)$$

The net transverse momentum of the produced heavy quark pair reflects the distribution of transverse momenta of the incoming partons and is therefore small.

1.3 Parton luminosities

Consider a generic hard process initiated by two hadrons of momenta P_1 and P_2 and $S = (P_1 + P_2)^2$.

$$\sigma(S) = \sum_{i,j} \int_0^1 dx_1 \int_0^1 dx_2 f_i(x_1, \mu) f_j(x_2, \mu) \hat{\sigma}_{ij}(\alpha_S(\mu), x_1 P_1, x_2 P_2) \quad (1.22)$$

In many circumstances the flux of partons with a given invariant mass squared will play a major role in the determination of the cross section. It is therefore convenient to define a parton luminosity L as a function of $\tau = s/S$ where s is the invariant mass squared of the partons.

$$\tau \frac{dL_{ij}}{d\tau} = \frac{1}{1 + \delta_{ij}} \int_0^1 dx_1 dx_2 [(x_1 f_i(x_1, \mu) x_2 f_j(x_2, \mu)) + (1 \leftrightarrow 2)] \delta(\tau - x_1 x_2) \quad (1.23)$$

Hence any parton cross section can be written as,

$$\sigma(S) = \sum_{i,j} \int_{\tau_0}^1 \frac{d\tau}{\tau} \left[\mathcal{L}_{ij}(\tau, s) \right] \left[s \sigma_{ij} \right] \quad (1.24)$$

$$\mathcal{L}_{ij}(\tau, s) = \left[\frac{\tau}{s} \frac{dL_{ij}}{d\tau} \right] \quad (1.25)$$

where $s = x_1 x_2 S$. \mathcal{L} has the dimensions of a cross-section. The second object in square brackets in Eq. 1.24 is dimensionless. It is approximately determined by powers of the relevant coupling constants. Hence knowing the luminosities, we can roughly estimate cross-sections. For this purpose we show the parton luminosities for gg , $u\bar{u}$ and $d\bar{d}$ in Figs. 4, 5 and 6. The luminosities are shown at the present energies of the CERN and FNAL $p\bar{p}$ colliders and at the energies of the proposed UNK collider ($\sqrt{S} = 6$ TeV, $p\bar{p}$), the LHC ($\sqrt{S} = 17$ TeV, pp) and the SSC ($\sqrt{S} = 40$ TeV, pp).

As an example of the use of these plots we examine the flux of partons with $\sqrt{s} = 100$ GeV. Since for heavy quark production $s \approx 4m_T^2$ this value is appropriate for the production of a quark of mass $m \approx 35$ GeV. From Figs. 4, 5 and 6 we find that,

$$\begin{aligned} \mathcal{L}_{gg} &= 1 \times 10^4 \text{ pb}, & \mathcal{L}_{u\bar{u}} &= 1.5 \times 10^4 \text{ pb}, & \mathcal{L}_{d\bar{d}} &= 2 \times 10^3 \text{ pb}, & \sqrt{s} &= 0.63 \text{ TeV} \\ \mathcal{L}_{gg} &= 3 \times 10^5 \text{ pb}, & \mathcal{L}_{u\bar{u}} &= 5 \times 10^4 \text{ pb}, & \mathcal{L}_{d\bar{d}} &= 2 \times 10^4 \text{ pb}, & \sqrt{s} &= 1.8 \text{ TeV} \end{aligned} \quad (1.26)$$

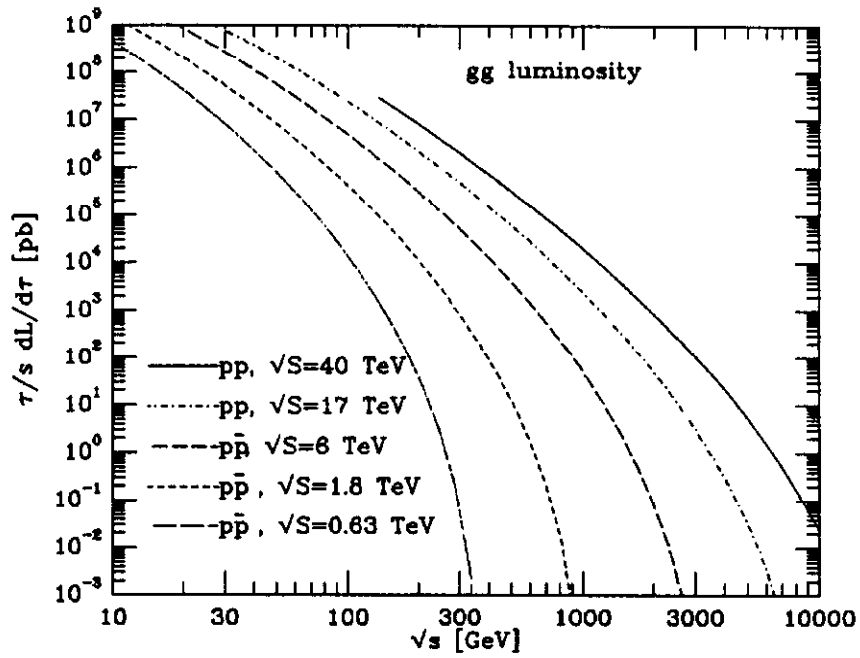


Figure 4: Luminosity plot for gluon-gluon.

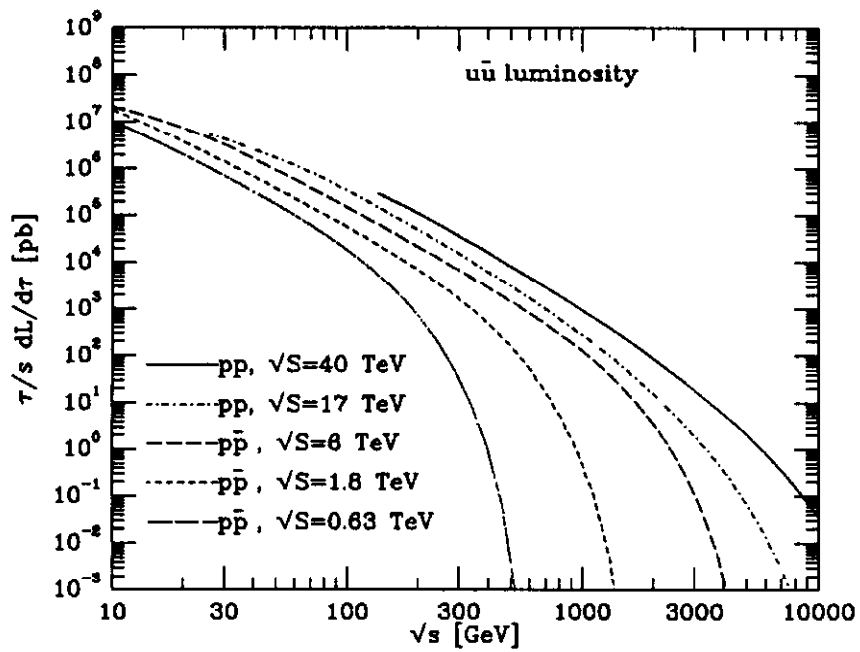


Figure 5: Luminosity plot for up quark-up antiquark.

Note that \mathcal{L}_{gg} is about 30 times larger at the Tevatron than at the CERN $S\bar{p}\bar{p}S$. The quark-antiquark luminosities at CERN are about the same size as the gluon-gluon luminosity, whereas they are a factor of ten smaller than the gluon-gluon luminosities at the Tevatron. We conclude that the production of a 35 GeV top quark at the Tevatron is dominated by gluon-gluon fusion. At CERN energies both the gluon-gluon and the quark-antiquark mechanisms are important. The cross section is expected to be about 10 times bigger at FNAL than at CERN. The estimate for the cross section for the production of a 35 GeV heavy quark at the Tevatron is ($\alpha_S \approx 0.1$),

$$\sigma \approx \alpha_S^2 \times 3 \times 10^6 \text{ pb} \approx 3 \times 10^4 \text{ pb} \quad (1.27)$$

In later sections we shall see that this rough estimate is confirmed by a more detailed analysis.

1.4 Higher order corrections to heavy quark production

The lowest order terms presented above are the beginning of a systematic expansion in the running coupling.

$$\hat{\sigma}_{ij}(s, m^2) = \frac{\alpha_S^2(\mu)}{m^2} \mathcal{F}_{ij}\left(\rho, \frac{\mu^2}{m^2}\right) \quad (1.28)$$

Eq. 1.28 completely describes the short distance cross-section for the production of a heavy quark of mass m in terms of the functions \mathcal{F}_{ij} , where the indices i and j specify the types of the annihilating partons. The dimensionless functions \mathcal{F}_{ij} have the following perturbative expansion,

$$\mathcal{F}_{ij}\left(\rho, \frac{\mu^2}{m^2}\right) = \mathcal{F}_{ij}^{(0)}(\rho) + 4\pi\alpha_S(\mu) \left[\mathcal{F}_{ij}^{(1)}(\rho) + \bar{\mathcal{F}}_{ij}^{(1)}(\rho) \ln\left(\frac{\mu^2}{m^2}\right) \right] + O(g^4) \quad (1.29)$$

where ρ is defined in Eq. 1.16. The functions $\mathcal{F}_{ij}^{(1)}$ are completely known[11]. Examples of the types of diagrams which contribute to $\mathcal{F}_{ij}^{(1)}$ are shown in Fig. 7. The full calculation involves both real and virtual corrections. For full details I refer the reader to ref. [11]. The gluon-gluon contribution is also considered in ref. [12]. In order to calculate the \mathcal{F}_{ij} in perturbation theory we must perform both renormalisation and factorisation of mass singularities. The subtractions required for renormalisation and factorisation are done at mass scale μ . The dependence on μ of the non-leading order term is displayed explicitly in Eq. 1.29.

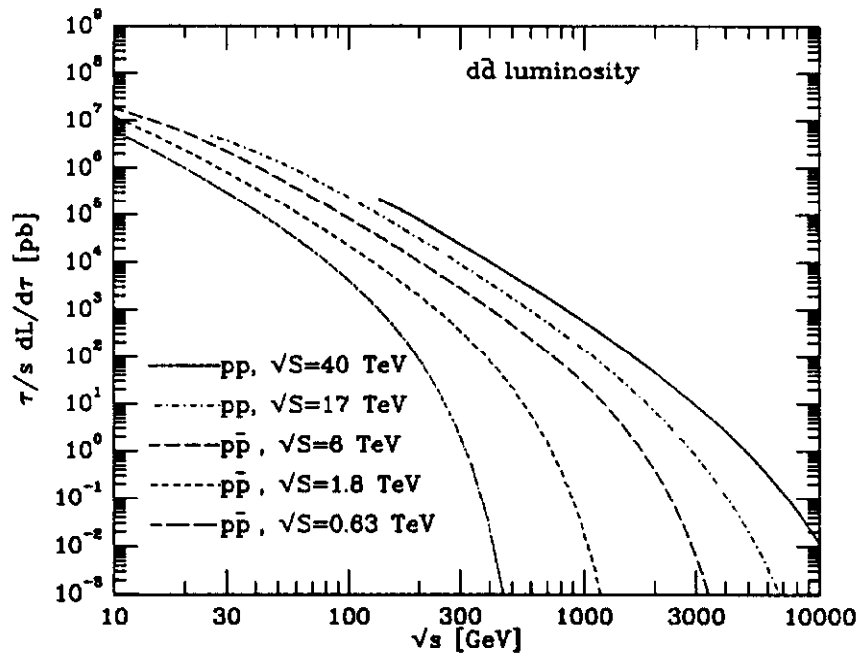


Figure 6: Luminosity plot for down quark-down antiquark.

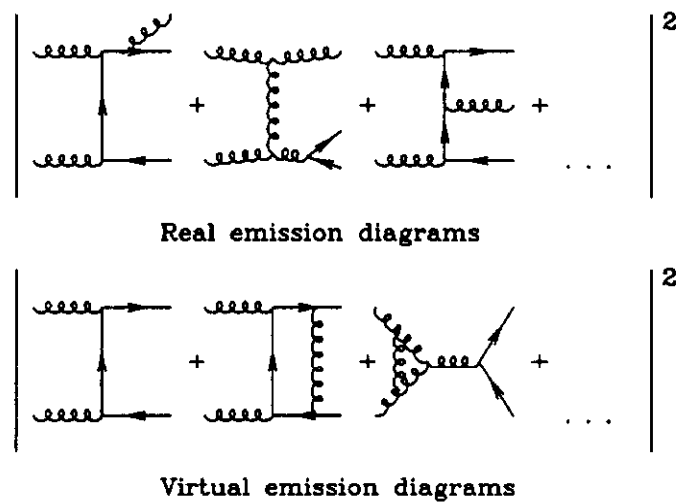


Figure 7: Examples of higher order corrections to heavy quark production.

Note that μ is an unphysical parameter. The physical predictions should be invariant under changes of μ at the appropriate order in perturbation theory. If we have performed a calculation to $O(\alpha_S^3)$, variations of the scale μ will lead to corrections of $O(\alpha_S^4)$.

$$\mu^2 \frac{d}{d\mu^2} \sigma = O(\alpha_S^4) \quad (1.30)$$

Using Eq. 1.30 we find that the term $\overline{\mathcal{F}}^{(1)}$ which controls the μ dependence of the higher perturbative contributions is fixed in terms of the lower order result $\mathcal{F}^{(0)}$.

$$\overline{\mathcal{F}}_{ij}^{(1)}(\rho) = \frac{1}{8\pi^2} \left[4\pi b \mathcal{F}_{ij}^{(0)}(\rho) - \int_{\rho}^1 dz_1 \mathcal{F}_{kj}^{(0)}\left(\frac{\rho}{z_1}\right) P_{ki}(z_1) - \int_{\rho}^1 dz_2 \mathcal{F}_{ik}^{(0)}\left(\frac{\rho}{z_2}\right) P_{kj}(z_2) \right] \quad (1.31)$$

In obtaining this result I have used the renormalisation group equation for the running coupling,

$$\begin{aligned} \mu^2 \frac{d}{d\mu^2} \alpha_S(\mu) &= -b\alpha_S^2(1 + b'\alpha_S + \dots) \\ b &= \frac{33 - 2n_f}{12\pi}, \quad b' = \frac{153 - 19n_f}{2\pi(33 - 2n_f)} \end{aligned} \quad (1.32)$$

and the Altarelli-Parisi equation,

$$\mu^2 \frac{d}{d\mu^2} f_i(x, \mu) = \frac{\alpha_S(\mu)}{2\pi} \sum_k \int_x^1 \frac{dz}{z} P_{ik}(z) f_k\left(\frac{x}{z}, \mu\right) \quad (1.33)$$

This illustrates an important point which is a general feature of renormalisation group improved perturbation series in QCD. The coefficient of the perturbative correction depends on the choice made for μ , but the μ dependence changes the result in such a way that the physical result is independent of the choice made for μ . Thus the μ dependence is formally small because it is of higher order in α_S . This does not assure us that the μ dependence is actually numerically small for all series. A pronounced dependence on μ is a signal of an untrustworthy perturbation series.

I shall illustrate this point by showing the μ dependence found in two cases of current interest. Firstly in Fig. 8, I show the μ dependence found for the hadroproduction of a 100 GeV top quark in leading and non-leading order. The inclusion of the higher order terms leads to a stabilisation of the theoretical prediction with respect to changes in μ . The situation for the bottom quark is quite different. In Fig. 9 the scale dependence of predicted bottom quark cross section is shown. The cross section

is approximately doubled by the inclusion of the higher order corrections, which do nothing to improve the stability of the prediction under changes of μ . It is apparent that the prediction of bottom production at collider energies is subject to considerable uncertainty.

I now turn to the question of flavour excitation. A flavour excitation diagram is one in which the heavy flavour is considered to reside already in the incoming hadron. It is excited by a gluon from the other hadron and appears on shell in the final state. An example of a flavour excitation diagram is shown in Fig. 10a. Note that in calculating the flavour excitation contribution the incoming heavy quark is treated as it were on its mass shell. If we denote the momentum transfer between the two incoming partons as q , the parton cross section will contain a factor $1/q^4$ coming from the propagator of the exchanged gluon. Therefore these graphs appear to be sensitive to momentum scales all the way down to the hadronic size scale. This casts doubt on the applicability of perturbative QCD to these processes.

In the following I shall sketch an analysis[8] which leads to an important conclusion. When considering the total cross section, flavour excitation contributions should not be included. The net contribution of these sorts of diagrams are already included as higher order corrections to the gluon-gluon fusion process. This analysis begins from the observation that the flavour excitation graph is already present as a subgraph of the first two diagrams shown in Fig. 10b. Does the flavour excitation approximation accurately represent the results of these diagrams? In particular is the $1/q^4$ pole, which is the signature of the presence of the flavour excitation diagrams, present in these diagrams?

I shall now indicate why the $1/q^4$ behaviour is not present in the sum of all three diagrams indicated in Fig. 10b. Let us denote the 'plus' and 'minus' components of any vector q as follows,

$$q^+ = q^0 + q^3, \quad q^- = q^0 - q^3, \quad q^2 = q^+q^- - q_T \cdot q_T \quad (1.34)$$

We choose the upper incoming parton in Fig. 10b to be directed along the 'plus' direction, $p_1 = p_1^+$. and the lower incoming parton to be directed along the 'minus' direction, $p_2 = p_2^-$. In the small q^2 region the 'plus' component of q is small, because

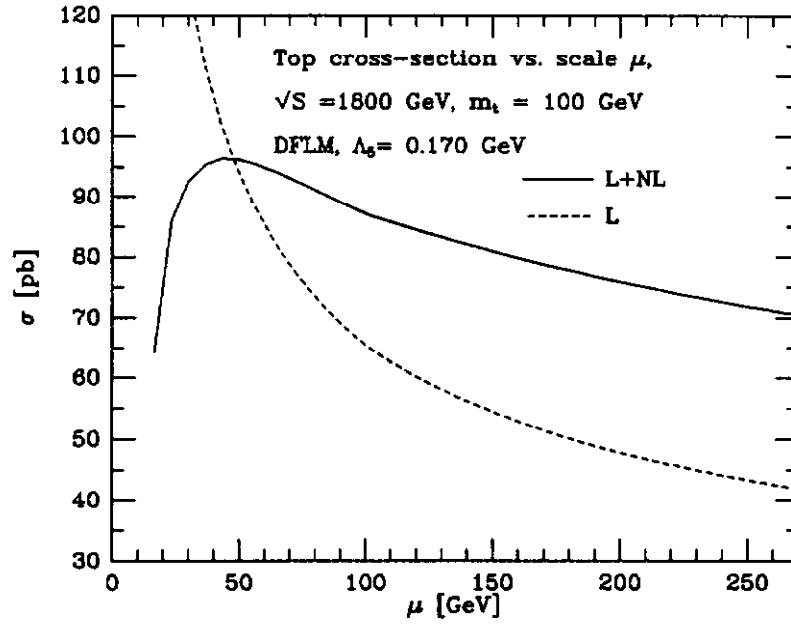


Figure 8: Scale dependence of the top quark cross section in second and third order.

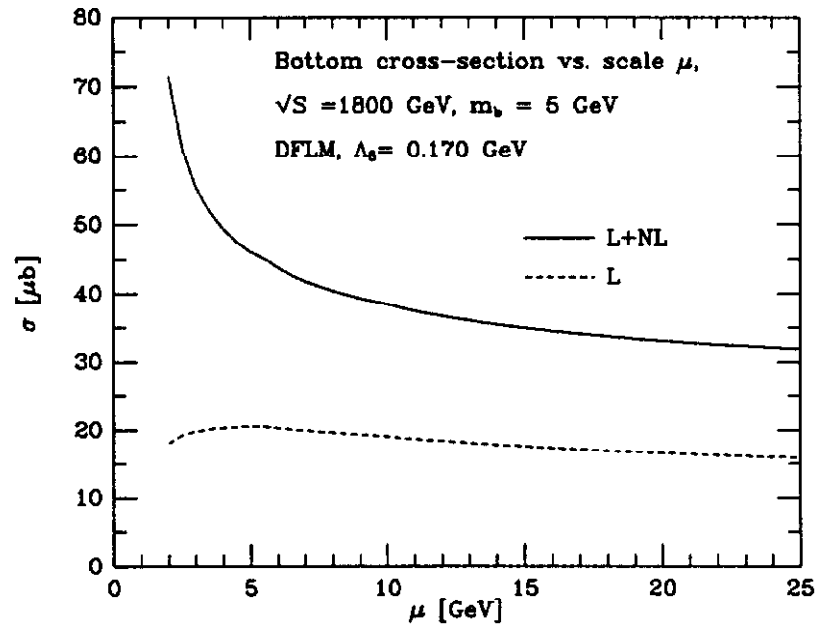
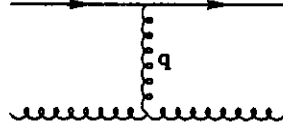
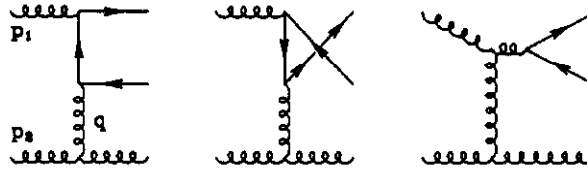


Figure 9: Scale dependence of the bottom quark cross section in second and third order.



a) Example of flavour excitation graph



b) Graphs containing spin-one exchange in the t-channel

Figure 10: Graphs relevant for discussion of flavour excitation.

the lower final state gluon is on shell.

$$(p_2 - q)^2 = 0, \quad q^+ = \frac{q^2}{2p_2^-} \tag{1.35}$$

since in the centre of mass system $p_1^+ \approx p_2^- \approx \sqrt{S}$. In the low q^2 region the ‘minus’ component of q is determined from the condition that production is close to threshold.

$$(p_1 + q)^2 \approx 4m^2, \quad q^- \approx \frac{m^2}{p_1^+} \tag{1.36}$$

q^- is therefore also small in the fragmentation region in which $p_1^+ \approx \sqrt{S}$. We therefore find that in the fragmentation region of upper incoming hadron,

$$q^2 = q^+ q^- - q_T \cdot q_T \approx -q_T \cdot q_T \tag{1.37}$$

The current J to which the exchanged gluon of momentum q couples is determined by the upper part of the three diagrams. In the fragmentation region only the ‘plus’

component is large.

$$q^\mu J_\mu = q^+ J^- + q^- J^+ - q_T \cdot J_T = 0, \quad J^+ \approx \frac{q_T \cdot J_T}{q^-} \quad (1.38)$$

where the Ward identity is a property of the sum of all three diagrams. The explicit term proportional to q_T in the amplitude shows that one power of the $1/q^2$ is cancelled in the amplitude squared.

This cancellation only occurs when the soft approximation to J^+ is valid. This requires the terms quadratic in q to be small compared to the terms linear in q in the denominators in the upper parts of the diagrams in Fig. 10b. The momentum q^- must not be too small.

$$q^2 < 2p^+ q^- \approx m^2 \quad (1.39)$$

We therefore expect the soft approximation to be valid and some cancellation to occur when $q^2 < m^2$. For further details I refer the reader to ref. [8]. The calculation of ref. [11] provides an explicit verification of this cancellation in the total cross section.

1.5 Heavy quarks in jets

A question of experimental interest is the frequency with which heavy quarks are found amongst the decay products of a jet. Since hadrons containing heavy quarks have appreciable semi-leptonic branching ratios such events will often lead to final states with leptons in jets. If we wish to use lepton plus jet events as a signature for new physics we must understand the background due to heavy quark production and decay.

This issue is logically unrelated to the total heavy quark cross section. As discussed above the total cross section is dominated by events with a small transverse energy of the order of the quark mass. Jet events inhabit a different region of phase space since they contain a cluster of transverse energy $E_T \gg m_c, m_b$. This latter kinematic region gives a small contribution to the total heavy quark cross section. A gluon decaying into a heavy quark pair must have a virtuality $k^2 > 4m^2$ so perturbative methods should be applicable for a sufficiently heavy quark. The number of $Q\bar{Q}$ pairs per gluon jet is calculable[13] using diagrams such as the one shown in Fig. 11. The calculation has two parts. Firstly one has to calculate $n_g(E^2, k^2)$, the number

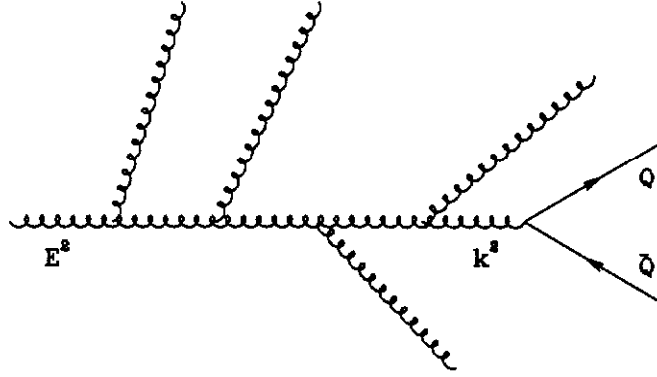


Figure 11: Heavy quark production in jets.

of gluons of off-shellness k^2 inside the original gluon with off-shellness E^2 . Secondly, one needs the transition probability of a gluon with off-shellness k^2 to decay to a pair of heavy quarks.

The number of gluons of mass squared k^2 inside a jet of virtuality E^2 is given by,

$$n_g(E^2, k^2) = \left[\frac{\ln(E^2/\Lambda^2)}{\ln(k^2/\Lambda^2)} \right]^a \frac{\exp \sqrt{[(2N_c/\pi b) \ln(E^2/\Lambda^2)]}}{\exp \sqrt{[(2N_c/\pi b) \ln(k^2/\Lambda^2)]}} \quad (1.40)$$

where

$$a = -\frac{1}{4} \left[1 + \frac{2n_f}{3\pi b} \left(1 - \frac{V}{2N_c^2} \right) \right] \quad (1.41)$$

and b is the first order coefficient in the expansion of the β function, Eq. 1.32. The correct calculation of the growth of the gluon multiplicity Eq. 1.40 requires the imposition of the angular ordering constraint which takes into account the coherence of the emitted soft gluons[14].

$R_{Q\bar{Q}}$ is the number of $Q\bar{Q}$ pairs per gluon jet. Ignoring for the moment gluon

branching calculated above, we obtain

$$R_{Q\bar{Q}} = \frac{1}{4\pi} \int_{4m^2}^{E^2} \frac{dk^2}{k^2} \alpha_S(k^2) \int_{z_-}^{z_+} dz \left[z^2 + (1-z)^2 + \frac{2m^2}{k^2} \right] \quad (1.42)$$

where the integration limits are given by $z_{\pm} = (1 \pm \beta)/2$ with $\beta = \sqrt{(1 - 4m^2/k^2)}$. The term $(z^2 + (1-z)^2)/2$ is recognisable as the familiar Altarelli-Parisi branching probability for massless quarks. Integrating over the longitudinal momentum fraction z we obtain,

$$R_{Q\bar{Q}} = \frac{1}{6\pi} \int_{4m^2}^{E^2} \frac{dk^2}{k^2} \alpha_S(k^2) \left[1 + \frac{2m^2}{k^2} \right] \sqrt{1 - \frac{4m^2}{k^2}} \quad (1.43)$$

The final result including gluon branching for the number of heavy quark pairs per gluon jet is,

$$R_{Q\bar{Q}} = \frac{1}{6\pi} \int_{4m^2}^{E^2} \frac{dk^2}{k^2} \alpha_S(k^2) \left[1 + \frac{2m^2}{k^2} \right] \sqrt{1 - \frac{4m^2}{k^2}} n_g(E^2, k^2) \quad (1.44)$$

The predicted number of charm quark pairs per jet is plotted in Fig. 12 using a value of $\Lambda^{(3)} = 300$ MeV and three values of the charm quark mass. Also shown plotted is the number of bottom quarks per jet with $\Lambda^{(4)} = 260$ MeV. The data point shows the number of D^* per jet as measured by the UA1 collaboration[15] and by the CDF collaboration[16]. In order compare these numbers with the $c\bar{c}$ pair rates, a model of the relative rates of D and D^* production is needed. For example, if all spin states are produced equally one would expect the charged D^* rate to be 75% of the total D production rate. The points in Fig. 12 needed to corrected upward for unobserved modes before they can be compared with the curves for the total $c\bar{c}$ pair rate.

2. Lecture 2

2.1 Phenomenological predictions

In this second lecture I will illustrate the application of Eqs. 1.1 and 1.2 to the production of hadrons containing heavy quarks. It is evident that in order to have a reliable estimate of the cross section one needs information on the running coupling,

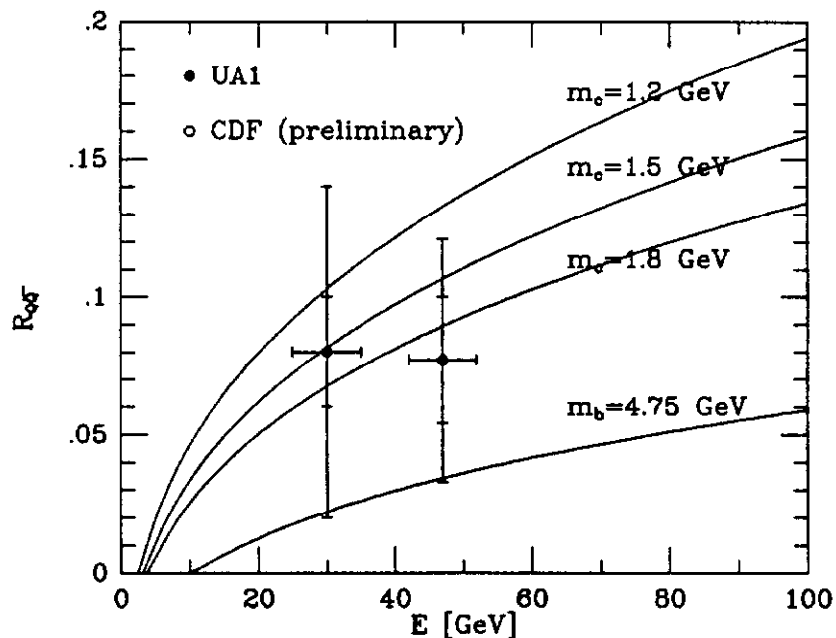


Figure 12: Heavy quarks in jets compared with UA1 and CDF data.

the form of the parton distributions and a calculation of the short distance cross section as a perturbation series in the coupling constant.

To give an idea of the order of magnitude uncertainty to be expected in these estimates, I show a partial compilation[17] of coupling constant measurements in Fig. 13. Also shown plotted is the expected theoretical form for several values of the QCD parameter Λ . By convention α_S is determined from the QCD parameter Λ by the following solution of Eq. 1.32.

$$\alpha_S(\mu) = \frac{1}{b \ln(\mu^2/\Lambda^2)} \left[1 - \frac{b' \ln \ln(\mu^2/\Lambda^2)}{b \ln(\mu^2/\Lambda^2)} + \dots \right]. \quad (2.1)$$

b and b' , which are also given in Eq. 1.32, depend on the number of active light flavours. Consequently Λ also depends on the number of active flavours. The relationship between the values of Λ for different numbers of flavours can be determined by imposing the continuity of α_S at the scale $\mu = m$, where m is the mass of the heavy quark. Here Λ is the QCD parameter in the \overline{MS} renormalisation scheme with five active flavours. It is apparent from Fig. 13, that the value of α_S is still subject to a considerable uncertainty. For definiteness I shall consider Λ to lie in the following

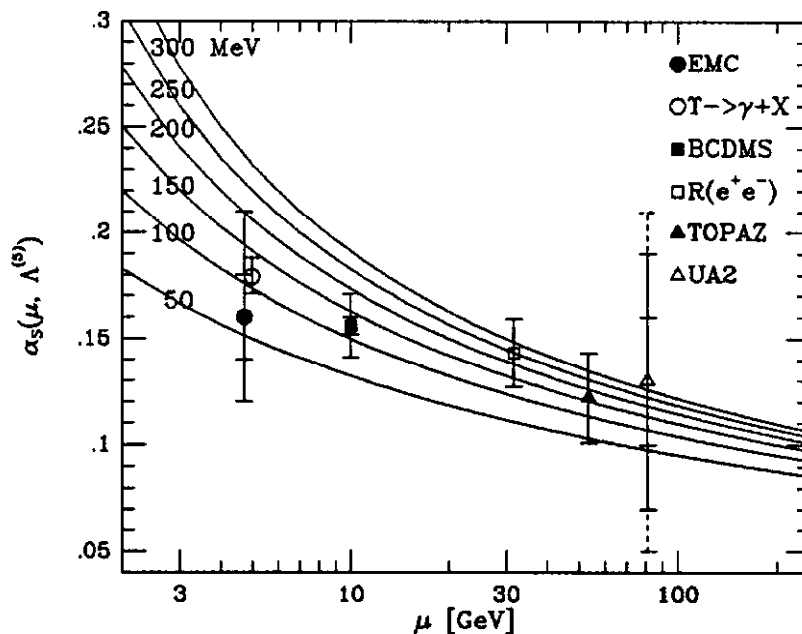


Figure 13: Behaviour of the running coupling.

range,

$$100 \text{ MeV} < \Lambda^{(5)} < 250 \text{ MeV} \quad (2.2)$$

but clearly other less restrictive interpretations of the data are possible. With this spread in the value of Λ the variation of α_S at $\mu = 100$ GeV is as follows,

$$0.104 < \alpha_S(\mu = 100 \text{ GeV}) < 0.118 \quad (2.3)$$

The uncertainty in α_S is larger at lower values of μ . It appears squared in any estimate of the heavy quark cross section.

The extraction of Λ from deep inelastic scattering is correlated with the form assumed for the gluon distribution function. A given set of data can be described by a stiff gluon distribution function and a large value of Λ , or by a softer gluon distribution and a smaller value of Λ . In order to make an estimate of the uncertainty due to the form of the gluon distribution function, I shall use three sets of distribution functions due to Diemoz, Ferroni, Longo and Martinelli[18]. These distribution functions have $\Lambda^{(5)} = 100, 170$ and 250 MeV and appropriately correlated gluon distribution functions.

The value of the heavy quark mass is the principal parameter controlling the size of the cross section. This dependence is much more marked than the $1/m^2$ dependence in the short distance cross section expected from Eq. 1.14. As the mass decreases, the value of x at which the structure functions must be supplied becomes smaller (*cf.* Eq. 1.9) and the cross section rises because of the growth of the parton flux.

The approach which I shall take to the estimate of theoretical errors in heavy quark cross sections is as follows[19]. I shall take Λ to run in the range given by Eq. 2.2 with corresponding variations of the gluon distribution function. I shall arbitrarily choose to vary the parameter μ in the range $m/2 < \mu < 2m$ to test the sensitivity to μ . Lastly, I shall consider quark masses in the ranges,

$$\begin{aligned} 1.2 < m_c < 1.8 \text{ GeV} \\ 4.5 < m_b < 5.0 \text{ GeV} \end{aligned} \tag{2.4}$$

I shall consider the extremum of all these variations to give an estimate of the theoretical error.

We immediately encounter a difficulty with this procedure in the case of charm. Variations of μ down to $m/2$ will carry us into the region $\mu < 1 \text{ GeV}$ in which we certainly do not trust perturbation theory. A estimate of the theoretical error on charm production cross sections is therefore not possible. In preparing the curve for charm production I have taken the lower limit on μ variations to be 1 GeV.

The dependence on the value chosen for the heavy quark mass is particularly acute for the case of charm. In fact, variations due to plausible changes in the quark mass, Eq. 2.4, are bigger than the uncertainties due to variations in the other parameters. I shall therefore take the aim of studies of the hadroproduction and photoproduction of charm to be the search for an answer to the following question. Is there a reasonable value for the charm quark mass which can accommodate the majority of the data on hadroproduction? In Fig. 14 I show the theoretical prediction for charm production. Note the large spread in the prediction. Also shown plotted is a compilation of data taken from ref. [20] which suggests that a value of $m_c = 1.5 \text{ GeV}$ gives a fair description of the data on the hadroproduction of D 's. After inclusion of the $O(\alpha_s^3)$ corrections, the data can be explained without recourse to very small values of the charmed quark mass[19].

This conclusion is further reinforced by consideration of the data on photoproduction of charm. The higher order corrections to photo-production $O(\alpha\alpha_s^2)$ have been considered in ref. [21]. After inclusion of these higher order terms we obtain predictions for the total cross section as a function of the energy of the tagged photon beam. The principal uncertainty derives from the value of the heavy quark mass, so I have plotted the minimum cross section which is obtained by varying Λ and the scale μ within the range $1 \text{ GeV} < \mu < 2m$ for three values of the charm quark mass. The comparison with the data on the photoproduction of charm [22,23], shown in Fig. 15, indicates that charm quark masses smaller than 1.5 GeV do not give an acceptable explanation of the data.

In conclusion within the large uncertainties present in the theoretical estimates, the D/\bar{D} production data presented here can be explained with a mass of the order of 1.5 GeV. This is not true of all data on the hadroproduction of charm, especially the older experiments. For a review of the experimental situation I refer the reader to ref. [24].

2.2 Results on the production of bottom quarks

The theoretical prediction of bottom quark production is very uncertain at collider energies. This has already been briefly mentioned in the discussion of Fig. 9. The cause of this large uncertainty is principally the very small value of x at which the parton distributions are probed. In fact, at present collider energies the bottom cross section is sensitive to the gluon distribution function at values of $x < 10^{-2}$. Needless to say the gluon distribution function has not been measured at such small values of x . An associated problem is the form of the short distance cross section in the large s region. The lowest order short distance cross sections, $\mathcal{F}^{(0)}$, given in Eq. 1.17, tend to zero in the large s region. This is a consequence of the fact that they also involve at most spin $\frac{1}{2}$ exchange in the t -channel as shown in Fig. 2. The higher order corrections to gg and gq processes have a different behaviour because they involve spin 1 exchange in the t -channel. The relevant diagrams are shown in Fig. 10b. In the high energy limit they tend to a constant [11]. Naturally these high s contributions are damped by the small number of energetic gluons in the parton flux, but at collider energies the region $\sqrt{s} \gg m$ makes a sizeable contribution to bottom cross section. The fact that this constant behaviour is present in both $\mathcal{F}^{(1)}$ and $\bar{\mathcal{F}}^{(1)}$ indicates the sensitivity of

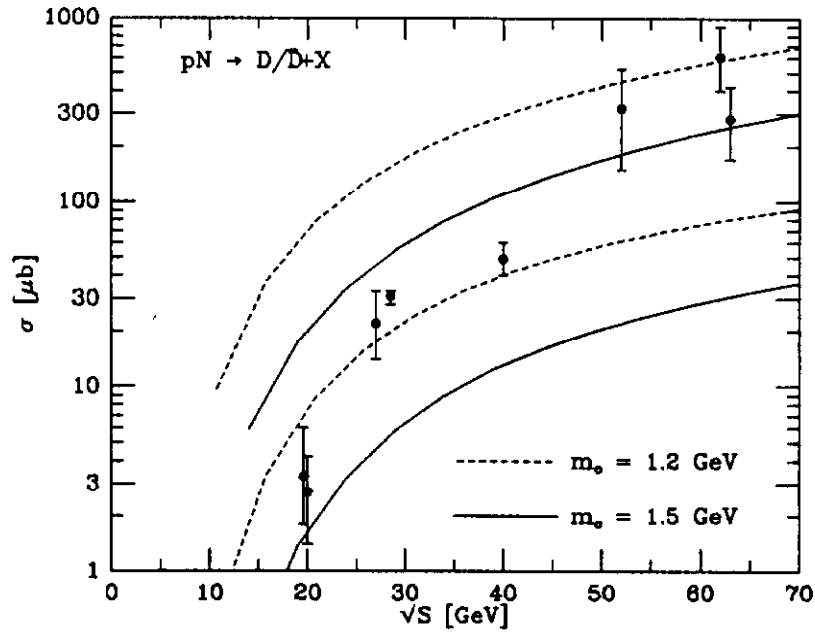


Figure 14: Data on hadroproduction of D/\bar{D} compared with theory.

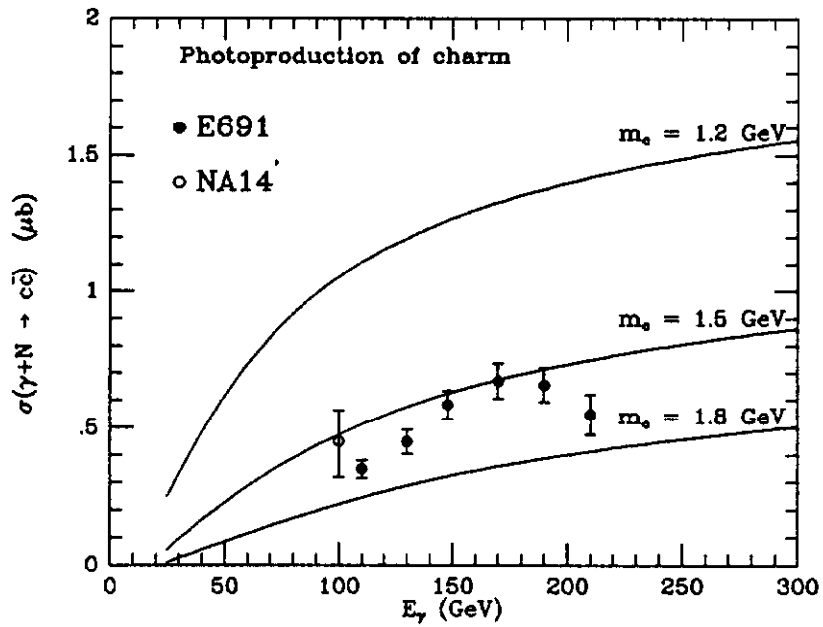


Figure 15: Data on photoproduction of charm compared with theoretical lower limits.

m_b [GeV]	σ (theory)	Theoretical error	Experimental data
$\sqrt{S} = 41$ GeV, pp			
4.5	23 nb	+21 -15	
5.0	9 nb	+8.4 -5.9	
$\sqrt{S} = 62$ GeV, pp			
4.5	142 nb	+98 -80	BCF[26], $150 < \sigma < 500$ nb
5.0	66 nb	+47 -38	
$\sqrt{S} = 630$ GeV, $p\bar{p}$			
4.5	19 μ b	+10 -8	UA1[27], 10.2 ± 3.3 μ b
5.0	12 μ b	+7 -4	
$\sqrt{S} = 24.5$ GeV, πN			
4.5	7.6 nb	+4.7 -3.8	WA78[28], $\sqrt{S} = 24.5$ GeV, $2 \pm 0.3 \pm 0.9$ nb
5.0	3.1 nb	+1.5 -1.5	NA10[29], $\sqrt{S} = 23$ GeV, $14 + 7 - 6$ nb

Table 2: Cross section for bottom production at various energies.

the size of this term to the value chosen for μ . There is therefore an interplay between the size of this term and the small x behaviour of the gluon distribution function.

At fixed target energies the cross section for the production of bottom quarks is theoretically more reliable. The μ dependence plot has a characteristic form similar to Fig. 8 and it is possible to make estimates of the theoretical errors. A compilation of theoretical results[25] and estimates of the associated theoretical error is shown in Table 2. The experimental study of the production of bottom quarks in hadronic reactions is still in its infancy, but Table 2 also includes the limited number of experimental results on total bottom production cross sections.

The calculations of ref. [11] also allow us to examine the p_T and rapidity distributions of the one heavy quark inclusive cross sections. Although the prediction of the total cross section at collider energy is uncertain, it is plausible that the shape of the transverse momentum and rapidity distributions is well described by the form found in lowest order perturbation theory. The supporting evidence[30] for this conjecture is shown in Fig. 16, which demonstrates that the inclusion of the first non-leading correction does not significantly modify the shape of the transverse momentum and rapidity distributions. At a fixed value of μ , the two curves lie on top of one another

if the lowest order is multiplied by a constant factor. Similar results hold also for the shape of the top quark distribution[30]. The UA1 collaboration have provided experimental information on the transverse distribution of the produced bottom quarks. In Fig. 17 comparison of the full α_s^3 prediction with UA1 data is made. The data is plotted as a function of the lower cutoff on the transverse momentum of the b quark. At lower values of k the agreement is satisfactory, but the experimental points lie somewhat above the theoretical curve at high k . It would be nice to have an independent confirmation of this experimental result. An inability to predict the value of the bottom cross section for large transverse momenta p_T , casts doubt on our ability to predict the top quark cross section for $m_t \approx p_T$. However in view of the difficulties of the experimental analysis, this discrepancy is probably not yet a cause for alarm.

The corresponding prediction for the shape of the bottom production cross section at the Tevatron is shown in Fig. 18.

2.3 Decays of the top quark

Consider first of all the decay of a very massive top quark which decays into an on-shell W -boson and a b -quark. The process has a semi-weak rate. In the limit in which $m_t \gg m_W$ the width is given by,

$$\Gamma(t \rightarrow bW) = \frac{G_F m_t^3}{8\pi\sqrt{2}} |V_{tb}|^2 \approx 170 \text{ MeV} |V_{tb}|^2 \left(\frac{m_t}{m_W}\right)^3 \quad (2.5)$$

When the top quark is so heavy that the width becomes bigger than a typical hadronic scale the top quark decays before it hadronises. Mesons containing the top quark are never formed.

This should be compared with the conventional top quark decay for $m_t < m_W - m_b$ which is a scaled up version of μ decay,

$$\Gamma(t \rightarrow be\bar{\nu}) = \frac{G_F^2 m_t^5}{192\pi^3} |V_{tb}|^2 \approx 2.3 \text{ keV} |V_{tb}|^2 \left(\frac{m_t}{40\text{GeV}}\right)^5 \quad (2.6)$$

The top branching ratio to leptons is given in the simplest approximation by counting modes for the W decay. Assuming the decay channel to $t\bar{b}$ is forbidden because $m_t > m_W - m_b$, the branching ratio is given by counting over the decay

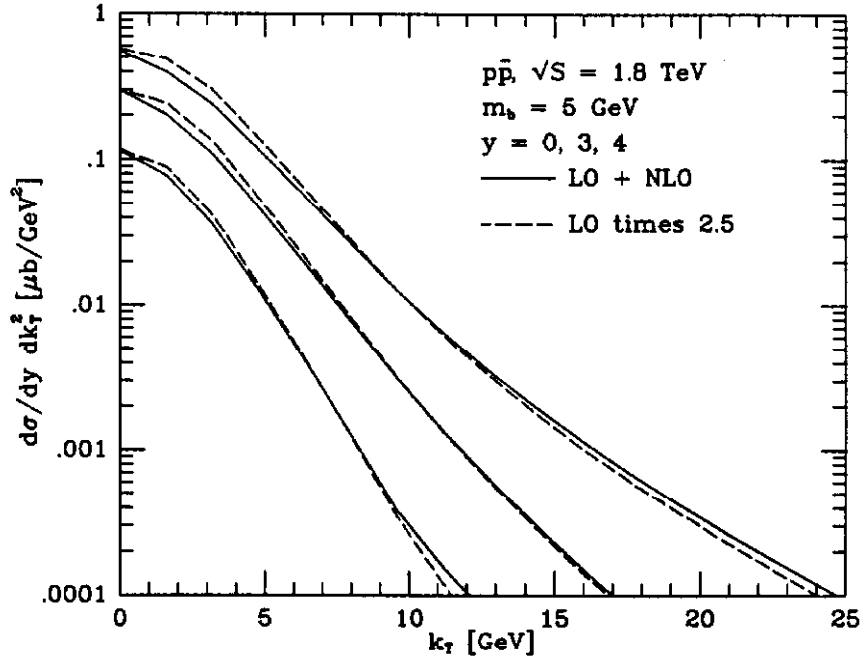


Figure 16: The shape of the cross-section for bottom quark production.

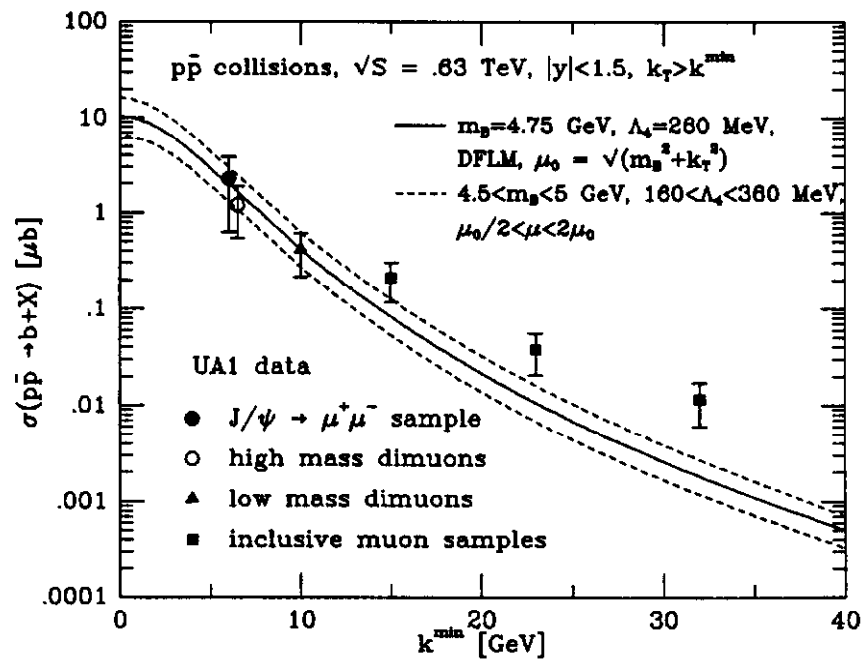


Figure 17: The cross-section for bottom quark production at CERN energy.

modes $e\bar{\nu}_e$, $\mu\bar{\nu}_\mu$, $\tau\bar{\nu}_\tau$ and three colours of $u\bar{d}$ and $c\bar{s}$.

$$\text{BR}(W^+ \rightarrow e^+\bar{\nu}) = \frac{1}{3+3+3} \approx 11\% \quad (2.7)$$

It is important to investigate unconventional decays of the top quark, especially if they alter the branching ratio into the leptonic decay mode. The leptonic decay mode is the basis of most searches for the top quark. A simple extension of the standard model involves the introduction of a second Higgs doublet. Top quark decay in this model has been investigated in ref. [31]. In order to avoid strangeness changing neutral currents[32] one must couple all quarks of a given charge to only one Higgs doublet. After spontaneous symmetry breaking we are left with one charged physical Higgs and three neutral Higgs particles. The dominant decay mode of the top quark is not to a leptonic mode, but rather to the charged Higgs,

$$\Gamma(t \rightarrow b\eta^+) > \frac{1}{4\pi v} \frac{m_b}{m_t^2} (m_t^2 + m_b^2 - m_\eta^2 + 2m_t m_b) \lambda(m_t, m_b, m_\eta) \quad (2.8)$$

where v is the normal vacuum expectation value and $\lambda(a, b, c) = \sqrt{(a^2 - b^2 - c^2)^2 - 4b^2c^2}$. In turn, the η^+ decays predominantly to $c\bar{s}$ and $\tau\nu_\tau$. If the vacuum expectation value of the two Higgs fields is taken to be equal the branching fraction into $c\bar{s}$ is found to be 64% and $\tau\nu_\tau$ is 31%[31].

2.4 The search for the top quark

The belief that the top quark must exist is based both on theoretical and experimental evidence. The theoretical motivation is that complete families are required for the cancellation of anomalies in the currents which couple to gauge fields. Hence the partner of the b, τ and ν_τ must exist to complete the third family.

An anomaly occurs in a theory because symmetries present at the classical level are destroyed by quantum effects. They typically involve contributions to the divergence of a current which is conserved at the classical level. If the gauge currents are anomalous, the Ward identities, which are vital for the proof that the gauge theory is renormalisable, are destroyed.

Anomalies occur in the simple triangle diagram with two vector currents and one axial vector current. Elimination of the anomalies for a particular current in the

lowest order triangle diagram is sufficient to ensure that the current remains anomaly free, even after the inclusion of more complicated diagrams. If the currents which interact at the three corners of the triangle couple to the matrices L^a, L^b and L^c for the left-handed fields, and to the matrices R^a, R^b and R^c for the right-handed fields, the vector-vector-axial vector triangle anomaly is proportional to,

$$A = \text{Tr} [R^a \{R^b, R^c\}] - \text{Tr} [L^a \{L^b, L^c\}]. \quad (2.9)$$

For the specific case of the $SU(2)_L \times U(1)$ theory of Weinberg and Salam we have the following weak isospin and hypercharge assignments for the third family ($Q = T_3 + Y$),

$$\begin{aligned} t_L, T_3 = \frac{1}{2}, Y_L = \frac{1}{6}, & \quad t_R, T_3 = 0, Y_R = \frac{2}{3}, \\ b_L, T_3 = -\frac{1}{2}, Y_L = \frac{1}{6}, & \quad b_R, T_3 = 0, Y_R = -\frac{1}{3}, \\ \nu_L, T_3 = \frac{1}{2}, Y_L = -\frac{1}{2} & \\ \tau_L, T_3 = -\frac{1}{2}, Y_L = -\frac{1}{2}, & \quad \tau_R, T_3 = 0, Y_R = -1 \end{aligned} \quad (2.10)$$

Substituting these couplings into Eq. 2.9, with all combinations of the $SU(2)$ matrices T^a or the $U(1)$ matrices Y we obtain the form of the anomaly for the gauge currents of the Weinberg-Salam theory. Two of the resulting traces of the couplings vanish for each fermion separately,

$$\text{Tr} T^a \{T^b, T^c\} = 0, \quad \text{Tr} T^a \{Y_L, Y_L\} = 0 \quad (2.11)$$

The other two traces vanish only for a complete family[34]

$$\text{Tr} (Y_R^3 - Y_L^3) = 0, \quad \text{Tr} Y_L \{T^a, T^b\} = 0 \quad (2.12)$$

It should be noted that there are still anomalies in global (non-gauged) currents in the Weinberg-Salam model. For example the normal isospin current corresponding to a global symmetry (in the absence of quark masses) is anomalous. It is this anomaly which is responsible for π^0 decay.

The experimental reason to believe in the existence of the top quark is the measurement of the weak isospin of the bottom quark. The forward backward asymmetry of b -jets in e^+e^- annihilation[33] is controlled by $a_e a_b$, the product of the axial vector

coupling to the electron and the b quark. The produced b and \bar{b} quarks are identified by the sign of the observed muons to which they decay. The measurement is therefore subject to a small correction due to $B^0 - \bar{B}^0$ mixing. Assuming that the axial coupling to the electron has its standard value the measured weak isospin of the left-handed b quark is [33],

$$T_3 = -0.5 \pm 0.1 \quad (2.13)$$

The simplest hypothesis is that the bottom quark is in an $SU(2)$ doublet with the top quark, although more complicated schemes are certainly possible.

Thus assured that the top quark exists, we must only find it. The expected cross section for the process

$$p + \bar{p} \rightarrow t + \bar{t} + X \quad (2.14)$$

is shown at in Fig. 19. The cross section is calculated using the full $O(\alpha_s^3)$ calculation of [11] and the method of theoretical error estimate described in the previous sections, (cf. [19]). In addition, production of top quarks through the decay chain $W \rightarrow t\bar{b}$ is also shown. Note the differing proportions of the two modes at CERN and FNAL energies. At $\sqrt{S} = 1.8(0.63)$ TeV the $t\bar{t}$ production is due predominantly due to gluon-gluon annihilation for $m_t < 100(40)$ GeV. On the other hand the W production comes mainly from $q\bar{q}$ annihilation at both energies. This explains the more rapid growth with energy of the $t\bar{t}$ production shown in Fig. 19.

From Fig. 19 the range of top quark masses which can be investigated in current experiments can be derived. In a sample of 5 inverse picobarns about 2500 $t\bar{t}$ pairs will be produced if the top quark has a mass of 70 GeV. One can observe the decays of the top quark to the $e\mu$ channel or to the $e + jets$ channel. With a perfect detector the numbers of events expected is,

$$\begin{aligned} \text{Number of } e\mu \text{ events} &= 2 \times .11 \times .11 \times 2500 \approx 50 \\ \text{Number of } e + \text{jet events} &= 2 \times .11 \times .66 \times 2500 \approx 300 \end{aligned} \quad (2.15)$$

The e plus jets channel gives a more copious signal and does not require muon detection, but the background is larger due to the process $p\bar{p} \rightarrow W + jets$. This background may become less severe with increasing top mass as the jets present in top decay become more energetic.

Let us assume that a limit of about 80 GeV will be set with the data from the 1988-1989 collider run. If the efficiency of extracting the signal from the data does not change with the mass of the top quark, we can expect to improve the limit by an additional 40 GeV above the present limit, by increasing the luminosity accumulated at the Tevatron by a factor of 10. Note however that the efficiency of the $e+$ multi-jets channels will increase for a heavier top quark. As the mass of the top quark increases the b quark jets occurring in its decay will be recognised in the detector as fully-fledged jets. This occurs with no extra price in coupling constants. The background due to normal W +jets production is suppressed by a power of α_S for every extra jet. It will become less important if we look in the channel with an electron and three and four jets.

References

- [1] R. P. Feynman, *Photon Hadron Interactions*, W. A. Benjamin, Reading, Mass (1972).
- [2] I. Hinchliffe, these proceedings.
- [3] R. K. Ellis, *Proceedings of the 1987 Theoretical Advanced Study Institute in Elementary Particle Physics*, edited by R. Slansky and G. West, (World Scientific).
- [4] G. Altarelli and G. Parisi, *Nucl. Phys.* **B126** (1977) 298 .
- [5] M. Gluck, J.F. Owens and E. Reya, *Phys. Rev.* **D17** (1978) 2324 ;
B. Combridge, *Nucl. Phys.* **151** (1979) 429 .
- [6] R. K. Ellis, *Strong Interactions and Gauge Theories*, edited by J. Tran Thanh Van, Editions Frontières, Gif-sur-Yvette, 1986, p. 339.
- [7] J. D. Bjorken and S. D. Drell, *Relativistic Quantum Fields*, McGraw Hill, New York (1964).
- [8] J. C. Collins, D. E. Soper and G. Sterman, *Nucl. Phys.* **B263** (1986) 37 .

- [9] S. J. Brodsky, J. C. Collins, S.D. Ellis, J. F. Gunion and A. H. Mueller, in *Proc. 1984 Summer Study on the Design and Utilization of the Superconducting Super Collider*, Fermilab, Batavia, Illinois, 1984, p. 227.
- [10] S. J. Brodsky, J. F. Gunion and D. E. Soper, *Phys. Rev. D* **36** (1987) 2710 .
- [11] P. Nason, S. Dawson and R. K. Ellis, *Nucl. Phys.* **B303** (1988) 607 .
- [12] W. Beenakker *et al.*, *Phys. Rev. D* **40** (1989) 54 .
- [13] A. H. Mueller and P. Nason, *Phys. Lett.* **157B** (1985) 226 .
- [14] A. Bassetto, M. Ciafaloni and G. Marchesini, *Phys. Rep.* **100** (1983) 201 and references therein.
- [15] M. Della Negra, Proceedings of the 6th topical workshop on proton antiproton collider physics, Aachen (1986).
- [16] F. Abe *et al.*, Fermilab preprint, Fermilab-PUB-89/171-E, (1989).
- [17] R. K. Ellis, Proceedings of the XXIV Conference on High Energy Physics, Munich, August 1988.
- [18] M. Diemoz *et al.*, *Zeit. Phys.* **C39** (1988) 21 .
- [19] G. Altarelli *et al.*, *Nucl. Phys.* **B308** (1988) 724 .
- [20] U. Gasparini, Proceedings of the XXIV Conference on High Energy Physics, Munich, August 1988.
- [21] R. K. Ellis and P. Nason, *Nucl. Phys.* **B312** (1989) 551 .
- [22] J. C. Anjos *et al.*, *Phys. Rev. Lett.* **62** (1989) 513 .
- [23] R. Forty, Proceedings of the XXIV Conference on High Energy Physics, Munich, August 1988.
- [24] S. P. K. Tavernier, *Rep. Prog. Phys.* **50** (1987) 1439 .
- [25] P. Nason, Proceedings of the XXIV Conference on High Energy Physics, Munich, August 1988.

- [26] L. Cifarelli *et al.*, (BCF collaboration) *Nucl. Phys. Proc. Suppl.* **1B** (1988) 55
- [27] C. Albajar *et al.*, *Zeit. Phys.* **C37** (1988) 505 ;
C. Albajar *et al.*, *Phys. Lett.* **B213** (1988) 405 .
- [28] M. G. Catanesi *et al.*, (WA78 collaboration), *Phys. Lett.* **202B** (1988) 453 .
- [29] P. Bordalo *et al.*, (NA10 collaboration), *Zeit. Phys.* **C39** (1988) 7 .
- [30] P. Nason, S. Dawson and R. K. Ellis, preprint FERMILAB-Pub-89/91-T, *Nucl. Phys. B* (in press).
- [31] S. Glashow and E. Jenkins, *Phys. Lett.* **196B** (1987) 233 .
- [32] S. Glashow and S. Weinberg, *Phys. Rev.* **D15** (1977) 1958 .
- [33] S. L. Wu, Proceedings of the Lepton Photon Symposium, Hamburg, August 1987;
W. Bartel *et al.*, *Phys. Lett.* **146B** (1984) 437
- [34] C. Bouchiat, J. Iliopoulos and P. Meyer, *Phys. Lett.* **38B** (1972) 519 ;
D. J. Gross and R. Jackiw, *Phys. Rev.* **D6** (1972) 477 .

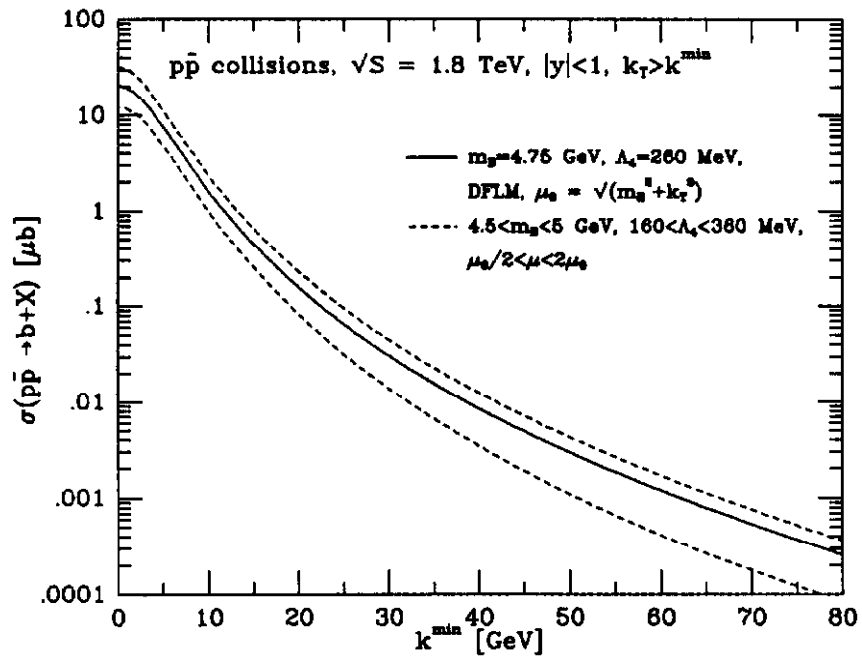


Figure 18: The cross-section for bottom quark production at FNAL energy.

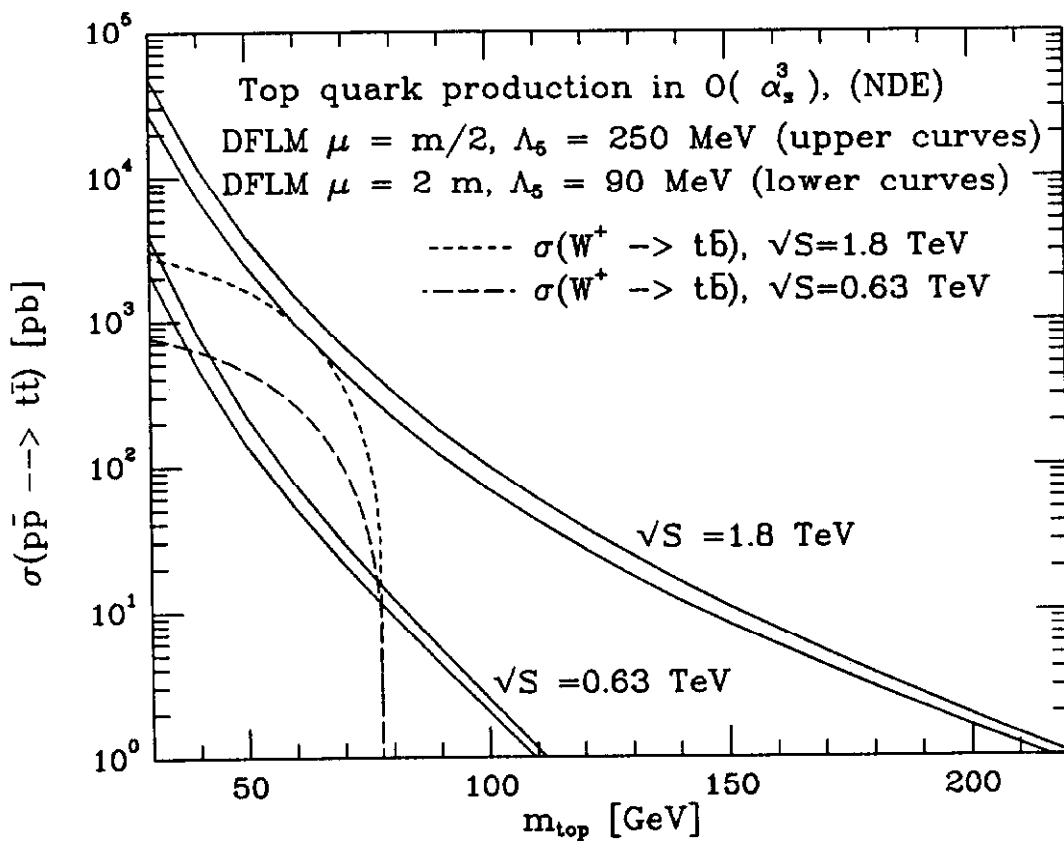


Figure 19: The cross section for top quark production at CERN and FNAL.